

Blood pressure in the Greenland shark as estimated from ventral aortic elasticity

Robert E. Shadwick¹, Diego Bernal², Peter G. Bushnell³, John F. Steffensen⁴

¹Department of Zoology, University of British Columbia, Vancouver, BC, Canada V6T 1Z4

²Department of Biology, University of Massachusetts, Dartmouth, MA 02747, USA

³Department of Biological Sciences, Indiana University South Bend, IN USA

⁴Marine Biological Section, University of Copenhagen, 3000 Helsingør, Denmark.

Abstract

We conducted *in vitro* inflations of freshly excised ventral aortas of the Greenland shark, *Somniosus microcephalus*, and used pressure-diameter data to estimate the point of transition from high to low compliance, which has been shown to occur at the mean blood pressure in other vertebrates including fishes. We also determined the pressure at which the modulus of elasticity of the aorta reached 0.4MPa, as occurs at the compliance transition in other species. From these analyses we predict the average ventral aortic blood pressure in *S. microcephalus* to be about 2.3-2.8kPa, much lower than reported for other sharks. Our results support the idea that this species is slow moving and has a relatively low aerobic metabolism. Histological investigation of the ventral aorta show that elastic fibres are present in relatively low abundance and loosely connected, consistent with this aorta to have high compliance at a relatively low blood pressure.

Introduction

Among lower vertebrates, including fishes, the degree of aerobic activity is reflected by the level of pressure generated by the heart. For example, tunas have high metabolic rates and are fast, continuous swimmers compared to other fishes such as trout or carp (Randall, 1970; Bernal et al., 2001; Brill and Lai, 2016). Not surprisingly, ventral aortic blood pressure in tunas (~12kPa, Bushnell and Brill, 1992; Jones et al., 2005) is more than three times higher than in trout, approaching levels in mammals (~13kPa, McDonald, 1974). Some sharks (e.g. catsharks) have relatively low activity, metabolic rate and blood pressures (3-5kPa; Taylor et al. 1977), while others (e.g. lamnid sharks) have higher metabolism and blood pressures (>7kPa; Lai et al., 1997) and the ability to swim fast.

Greenland sharks (*Somniosus microcephalus*) live in deep, cold water in high northern latitudes, grow to a large size (>5m), have a lifespan of hundreds of years (Hansen, 1963; Nielsen et al., 2016) and appear to be very sluggish with little capacity for sustained high speed swimming (Compagno et al., 2005; Watanabe et al., 2012, Nielsen et al., 2016). Although one of the largest extant marine fish, knowledge of their life history, ecology and physiology is very limited (MacNeil et al., 2012; Herbert et al., 2017, Costantini et al., 2017). There are virtually no *in vivo* measurements of physiological parameters from this species, due to the difficulty of obtaining and handling specimens. Field studies using accelerometers reveal very slow sustained swim speeds (< 0.2 body length s^{-1}), with tail beat frequencies on the order of only a few per minute (Skomal and Benz, 2004; Watanabe et al., 2012). Based on all these features we expect blood pressure in *S. microcephalus* to be relatively low compared to other sharks, even low-activity ones such as catsharks.

In animals with closed circulatory systems the major arteries act as an elastic reservoir, storing blood transiently when the ventricle contracts, and providing flow while the heart refills. Elastic recoil of the artery wall converts the pulsatile output of the heart into smoother flow in the periphery. In fish, the heart pumps blood to the gills through a highly compliant and elastic ventral aorta (VA). Studies have shown that the proximal aortas of vertebrates and some invertebrates all have nonlinear inflation curves. Commonly, the aorta is very compliant at low pressures but changes fairly abruptly to a stiff-walled vessel at higher pressures. Because of cylindrical geometry, this non-linear behaviour is necessary to prevent aneurysms, or pressure ruptures (Shadwick, 1999), and the transition in compliance typically occurs at about mean blood pressure of each species (Fig. 1A; Roach and Burton, 1957; Gosline 2018). This inherent elastic property provides a method to estimate mean blood pressure, and has been used for animals in which *in vivo* measurements are not available or are intractable (Gosline and Shadwick 1982; Shadwick 1995).

A variation of this method was developed for teleosts (Jones et al., 2005) using the bulbus arteriosus, an elastic chamber that connects the ventricle to the VA (Priede, 1976; Bushnell et al., 1992; Braun et al., 2003a,b). Jones et al. (2005) validated their method by showing good accord ($R^2=0.89$) between measured blood pressures and predictions from the inflation properties of the bulbi of ten species.

The elastic properties of the aortic wall arise from the combined effect of two distinct fibrous proteins, elastin and collagen. Elastin is highly extensible with a tensile stiffness (or elastic modulus) about equal to that of natural rubber (~ 1 MPa) while collagen is 1000 times stiffer (~ 1 GPa) and relatively inextensible. Compliance is initially associated with the high extensibility of elastin fibres that bear wall tension until distension of the artery is great enough to unfold and recruit the collagen fibres, resulting in a rapid increase in wall stiffness with pressure (Roach and Burton, 1957; Lillie et al., 2012). The

ratio of collagen to elastin provides an index of wall stiffness at physiological pressures in different species, but the total quantity and structural arrangement of the connective tissue fractions are also important in determining the artery mechanical properties, in particular its distensibility as a function of pressure. A consequence of this design feature is that, while the elastic modulus (stiffness) increases sharply with radial expansion, a value of 0.3-0.5MPa is consistently observed for the aorta at mean physiological pressure in a wide range of species (Gibbons and Shadwick, 1989; Shadwick, 1999). This observation provides a second method to estimate blood pressure from tissue mechanics.

The purpose of our study, then, was to estimate mean blood pressure in the Greenland shark from measurements of the elastic properties of the VA.

Methods

Ventral aortas were collected post-mortem from six Greenland sharks (*S. microcephalus*) that were captured by long-line fishing in Greenland waters during two research cruises (2012, 2017). Animals ranged in size from 2.64 to 3.7m total length, with body masses of approximately 170kg to 700kg.

Each VA was dissected free from adventitia and separated from the heart by sectioning at the outflow of the conus arteriosus, and from the gill complex by sectioning the afferent branchial vessels. During dissection, it was apparent that the VA was very elastic as there was significant recoil when the vessel was excised (average shortening measured *ex vivo* vs *in situ* of $38 \pm 7\%$). Next, a large cannula was inserted in the vessel proximal to the conus arteriosus and tied in with silk suture, and a smaller one was fitted to the distal outflow in the same manner (Fig.1B) along with a side arm to a calibrated pressure transducer. This left a relatively uniform segment 6-8cm in length between gill afferent vessels 3 and 4 where VA diameter could be monitored upon inflation (Fig.1B). Before inflation, the VA segment was extended longitudinally and held to restore its *in vivo* length.

Inflation tests were conducted by filling the VA with 4°C shark saline (Driedzic and Gesser, 1988) from a reservoir that was slowly hoisted over a pulley suspended from the ceiling. Before taking measurements, the VA was preloaded through several inflation cycles to approximately 6kPa. Pressure was monitored continuously by reading the DC voltage output of the amplified pressure transducer signal with a voltmeter. During the inflations, a video recording was made that included the VA and also the voltmeter. This allowed frame by frame determination of inflation pressure (P) and the corresponding VA external diameter (D). The latter was measured using ImageJ on video frames that were selected as the closest to a pressure series of 0 to 5 kPa in increments of 0.5kPa. Then, each D value was divided by the zero-pressure D to give a diameter ratio.

Following the inflation trials, a short ring was sliced from the VA at the location where D had been measured; this was turned on end and photographed in order to determine wall thickness (h), using ImageJ. This value represents the thickness of the unpressurized, unstretched vessel wall. Ring D averaged 1.27 ± 0.19 cm with an average h of 0.15 ± 0.03 cm. Based on the longitudinal stretch needed to restore *in vivo* length, h for the stretched vessel was first calculated at $P = 0$, and then at each selected inflation P , based on corresponding D and assuming constant volume of the vessel wall tissue (Shadwick and Gosline, 1985). From this, the internal radius (r) at each P increment was calculated. Then, circumferential wall stress was calculated as $P \times r/h$, and circumferential wall strain was calculated as the increment in mean wall radius divided by its initial value, where mean wall radius is $r + h/2$. Stress and strain increments were then used to calculate the stiffness, or incremental elastic modulus, of the VA as a function of inflation P (Eqns. 1-3, 12 in Shadwick and Gosline, 1985).

The artery wall structure was investigated by routine histological methods. Tissues were fixed in 4% formaldehyde buffered with filtered sea water, dehydrated through an ethanol series, embedded in wax and sectioned at $5 \mu\text{m}$. Sections were stained for connective tissue (collagen \rightarrow pink; elastin \rightarrow black) by the Verhoff-van Gieson method, viewed and photographed on a Zeiss Axio-Imager.A1 photomicroscope fitted with a Hitachi HV-F22 digital camera. Determinations of the relative elastin content were made by converting histological images of transverse and longitudinal sections to grayscale, then binary format using ImageJ software. With this method elastin remains as black (grayscale value = 255) while the rest of the colours are subtracted, leaving only white (grayscale value = 0). By finding the average grayscale value for each image we could calculate the fraction of pixels that were black, and thus the proportion of the section area that was occupied by elastin. For comparison, a VA obtained from a short-fin mako shark (*Isurus oxyrinchus*, ~70 kg body mass) was prepared and analysed in the same manner. Results are reported as mean \pm S.D.

Results and Discussion

Our first method of blood pressure estimation is based on inflation data for six Greenland shark ventral aortas (Fig.2A) showing the expected non-linear increase in P vs D . It is notable how readily the VA expands at very low pressures (i.e. < 2 kPa) before stiffening as pressure exceeds 2 kPa. Linear regressions are shown for the first five and last five data points. Their intersection marks the transition from compliant to stiff regions and defines the level that we regard as resting aortic blood pressure, as demonstrated previously for other animals (Roach and Burton, 1957). Here, this occurs at approximately 2.3 kPa.

An alternative estimation of blood pressure is based on the elastic modulus of the VA wall. Fig.2B shows that the circumferential elastic modulus increases as a nonlinear function of P , rising 100-fold between P of 0.5kPa and 4kPa. Fig.2C shows plots of the elastic modulus of the aorta from various vertebrates and invertebrates with closed circulatory systems vs. P , normalized to the known mean blood pressure (P_{mean}) of each species (Shadwick, 1999). While these species have greatly varying levels of blood pressure, the normalized data show, remarkably, that the aortic elastic modulus is consistently 0.3-0.5MPa at mean blood pressure in all species. If we assume this observation holds for the Greenland shark, then taking an average modulus of 0.4MPa, we predict a mean blood pressure of 2.8KPa in this species (Fig.2B).

Combining results from the two methods predicts mean ventral aortic blood pressure for *S. microcephalus* of 2.3-2.8kPa. We believe this is lower than blood pressures observed in any other elasmobranch, and fits with the expectations that this species is slow moving and has a relatively low aerobic metabolism (MacNeil et al., 2012; Watanabe et al. 2012). For comparison, *in vivo* studies report ventral aortic blood pressures from slow swimming sharks of 3.9 and 5.3kPa (epaulette shark, *Hemiscyllium ocellatum*; Speers-Roesch et al., 2012, and catshark, *Scyliorhinus canicula*; Taylor et al. 1977, respectively), from more active species of 5.1-6.8kPa (black-tipped reef shark, *Carcharhinus melanoptera*; Davie et al., 1993, and leopard shark, *Triakis semifasciata*; Lai et al. 1990), and from fast swimming sharks of >7kPa (short-fin mako sharks, *Isurus oxyrinchus*; Lai et al, 1997). As in other fishes, there is undoubtedly a significant pressure drop across the gills due to resistance, such that the dorsal aortic pressure will be even lower than we predict for the VA. In teleosts and other sharks this is typically a pressure decrease of about 25% (Stevens and Randall, 1967; Taylor et al., 1977; Stensl kken et al., 2004) suggesting that the systemic blood pressure in the Greenland shark may be below 2kPa.

The organization of the load-bearing fibrous connective tissues in the VA of *S. microcephalus* should reflect its observed capacity to inflate to a higher degree at lower pressures than other species. Histological features bear this out. The VA wall in *S. microcephalus* is composed primarily of collagen, elastin and smooth muscle cells (Fig.3A), organized in three distinct layers (intima, media, adventitia) reminiscent of what is seen in other vertebrate arteries (Shadwick, 1998; 1999). At the luminal surface the intima comprises an endothelial cell layer supported by an internal elastic lamina (Fig.3B,C). The media contains elastin fibres, smooth muscle cells and collagen fibres, while the adventitia is predominately loose collagen with scattered elastin fibres. An interesting feature of the media is a region about 50 m thick adjacent to the intima where elastin fibres and muscle cells are oriented parallel to the longitudinal vessel axis, whereas elastin and muscle cells in much of the rest of the media are oriented circumferentially. This can be seen by comparing longitudinal and circumferential

sections in Fig.3B,C, and sagittal sections in Fig.3E,F. This biaxial deposition of elastic fibres will provide resistance to stretching in both axes during pressurization *in vivo*.

In *S. microcephalus* the elastin complement is much more dispersed than in the aorta of other vertebrate species, including other fishes (Satchell, 1971; Rhodin, 1972; Gibbons and Shadwick, 1989; Braun et al, 2003a; Fig.3D). In transverse, longitudinal and sagittal sections, elastin is seen as fibres of 1-2 μ m or less in diameter (Fig.3B,C) rather than the fenestrated circumferential sheets seen in mammalian arteries (Wong and Langille, 1996; Clarke et al., 2015). This relatively loose connectivity of the fibres should allow a higher distensibility at low pressures compared to the mammalian arrangement (Gibbons and Shadwick, 1989). We determined that the area occupied by elastin in transverse and longitudinal sections averaged $27 \pm 2.5\%$. As a proxy for the volume fraction, this is about half of what is typical in mammalian aortas (Harkness et al., 1957; Roach and Burton, 1957). In a pressurized cylinder, circumferential wall tension is $P \times r$. If the tension up to mean blood pressure is resisted by the elastin component, then the wall extensibility at a given pressure will be relatively higher when elastin is low in abundance and loosely linked, as in *S. microcephalus*. Conversely, in species with higher blood pressures, due to the greater density and connectivity of elastin fibres in the aortic walls, higher pressures will be required to achieve the same aortic distension. Above the inflection point of the *P-D* curve collagen straightens and becomes the load bearing element in all cases (recall collagen is 1000 times stiffer than elastin). Thus, the distribution and organization of the connective tissues is the primary structural mechanism whereby the aorta of different species have similar functional properties across a wide range of species-specific blood pressures (Fig.2C). Remarkably, this pattern is also seen in the aorta of invertebrates with closed circulatory systems, such as cephalopods and crustaceans, where elastin analogues occur with collagen (Davison et al., 1995; McConnell et al., 1996; Shadwick, 1995, 1999; Shadwick and Gosline, 1981; Shadwick et al., 1990). These observations suggest that cellular control of the deposition of collagen and elastic fibre components may be related to the level of pressure experienced during growth and development of the circulatory system, specific to each species.

For comparison to *S. microcephalus*, we analysed a VA from the highly active short-fin mako shark. In this case, the VA wall has a much denser complement of elastin fibres (Fig.3D) with an average elastin area of $53 \pm 2.6\%$, about double that of *S. microcephalus*, and its mean blood pressure (ca. 7kPa) is substantially higher (Lai et al., 1997).

In this study we used two methods to estimate the ventral aortic blood pressure of the enigmatic Greenland shark, based on artery wall mechanics. Together these yield predictions of 2.3-2.8kPa, much lower than other shark species in which blood pressure has been measured. This low value for arterial pressure is not unexpected, considering the apparent low level of aerobic activity observed in this species, and this prediction is supported by the microscopic arrangement of elastin and collagen in the VA wall.

Acknowledgements

Data in this study were collected on two research cruises funded by the Danish Centre for Marine Research, The Carlsberg Foundation and the Danish Council for Independent Research, under permits from Greenland Home Rule (Akt. Nr.2017-9208). RS was supported by Discovery and Accelerator Supplement Grants from the Natural Sciences and Engineering Research Council of Canada (RGPIN 312039-13 and RGPAS 446012-13, respectively). DB was supported by the National Science Foundation under grant IOS-1354593. Any opinions, findings, and conclusions or recommendations expressed in this material are those of the author(s) and do not necessarily reflect the views of the National Science Foundation

References

- Bernal, D. Dickson, K.A., Shadwick, R.E. and Graham, J.B. (2001). Analysis of the evolutionary convergence for high performance swimming in lamnid sharks and tunas. *Comp. Biochem. Physiol. A* 29: 695-726.
- Braun, M.H., Brill, R.W., Gosline, J.M. and Jones, D.R. (2003a). Form and function of the bulbus arteriosus in yellowfin tuna (*Thunnus albacares*), bigeye tuna (*Thunnus obesus*) and blue marlin (*Makaira nigricans*): static properties. *J. Exp. Biol.* 206: 3311-3326.
- Braun, M.H., Brill, R.W., Gosline, J.M. and Jones, D.R. (2003b). Form and function of the bulbus arteriosus in yellowfin tuna (*Thunnus albacares*): dynamic properties. *J. Exp. Biol.* 206: 3327-3335.
- Brill, R.W. and Lai, N.C. (2016). Elasmobranch Cardiovascular System. *Fish Physiology*, (Eds. R.E. Shadwick, C.J. Brauner, A.P. Farrell) 34B: 1–82.
- Bushnell, P.G. and Brill, R.W. (1992). Oxygen transport and cardiovascular responses in skipjack (*Katsuwonus pelamis*) and yellowfin tuna (*Thunnus albacares*) exposed to acute hypoxia. *J. Comp. Physiol.* 162:131-143.
- Bushnell, P.G., D.R. Jones, and Farrell, A.P. (1992). The arterial system. In: "*Fish Physiology, Vol XII. Respiratory and Cardiovascular Control*". (W.S. Hoar, D.J. Randall and A.P. Farrell, eds.). Academic Press, N.Y. pp. 89-139.
- Clarke, T.E., Lillie, M.A., Vogl, A.W., Gosline, J.M. and Shadwick, R.E. (2015) Mechanical contribution of lamellar and interlamellar elastin along the mouse aorta. *J. Biomech.* 48: 3608-3614.
- Compagno, L.J.V., Dando, M. and Fowler, S. (2005). *Sharks of the World*. Princeton University Press, Princeton, N.J. USA.
- Costantini, D., Smith, S., Killen, S, Nielsen, J. and Steffensen, J.F. (2017). The Greenland shark: A new challenge for the oxidative stress theory of ageing? *Comp. Biochem. Physiol. A: Molec. & Integ. Physiol.* 203: 227-232.
- Davie, P.S., Franklin, C.E. and Grigg, G.C. (1993). Blood pressure and heart rate during tonic immobility in the black tipped reef shark, *Carcharhinus melanoptera*. *Fish Physiol. Biochem.* 12: 95-100.
- Davison, I.G., Wright, G.M. and Demont, M.E. (1995). The structure and physical properties of invertebrate and primitive vertebrate arteries. *J. Exp. Biol.* 198: 2185-2196.
- Driedzic, W.R. and Gesser, H. (1988). Differences in force-frequency relationships and calcium dependency between elasmobranch and teleost hearts. *J. Exp. Biol.* 140: 227-241.
- Gabella, M.A., Jacob, C.T., Raya, T.E., Liu, J., Simon, B. and Goldman, S. (1998). Large artery remodeling during aging. Biaxial passive and active stiffness. *Hypertension* 32:437-443.

- Gibbons, C.A. and Shadwick, R.E. (1989). Functional similarities in the mechanical design of the aorta in lower vertebrates and mammals. *Experientia* 45: 1083–1088.
- Gibbons, C.A. and Shadwick, R.E. (1991). Circulatory mechanics in the toad *Bufo marinus*: I. Structure and mechanical design of the aorta. *J. Exp. Biol.* 158: 275–289.
- Gosline, J.M. (2018). *Mechanical design of structural materials in animals*. Princeton Press.
- Gosline, J.M. and Shadwick, R.E. (1982). The biomechanics of the arteries of *Nautilus*, *Notodarus* and *Sepia*. *Pacif. Sci.* 36: 283–296.
- Hansen, P.M. (1963). Tagging experiments with the Greenland shark (*Somniosus microcephalus* (Bloch and Schneider)) in Subarea 1. *International Commission Northwest Atlantic Fisheries Special Publication* 4: 172–175.
- Harkness, M.L.R., Harkness, R.D. and McDonald, D.A. (1957). The collagen and elastin content of the arterial wall in the dog. *Proc. Roy. Soc. B.* 146: 541–551.
- Herbert, N.A., Skov, P.V., Tirsgaard, B. Bushnell, P.G., Brill, R.W., Harvey Clark, C. and Steffensen, J.F. (2017). Blood O₂ affinity of a large polar elasmobranch, the Greenland shark *Somniosus microcephalus*, *Polar Biol.* 40: 2297–2305.
- Jones, D.R., Perbhoo, K. and Braun, M.H. (2005). Necrophysiological determination of blood pressure in fishes. *Naturwissenschaften* 92: 582–585.
- Lai, N.C., Graham, J.B. and Burnett, L. (1990). Blood respiratory properties and the effect of swimming on blood gas transport in the leopard shark *Triakis semifasciata*. *J. Exp. Biol.* 151: 161–173.
- Lai, N.C., Korsmeyer, K.E., Katz, S., Holts, D.B., Laughlin, L.M. and Graham, J.B. (1997). Hemodynamics and blood properties of the shortfin mako shark (*Isurus oxyrinchus*). *Copeia* 1997: 424–429.
- Lillie, M.A., Armstrong, T.E., Gerard, S.G., Shadwick, R.E. and Gosline, J.M. (2012). Contribution of elastin and collagen to the inflation response of the pig thoracic aorta: Assessing elastin's role in mechanical homeostasis. *J. Biomech.* 45: 2133–2141.
- MacNeil, M.A. McMeans, B.C., Hussey, N.E., Vecsei, P., Svavarsson, J., Kovacs, K.M., Lydersen, C., Treble, M.A., Skomal, G.B. Ramsey, M. and Fisk, A.T. (2012). Biology of the Greenland shark *Somniosus microcephalus*. *J. Fish Biol.* 80: 991–1018.
- McConnell, C.J., Wright, G.M. and DeMont, M.E. (1996). The modulus of elasticity of lobster aorta microfibrils. *Experientia* 52: 918–921.
- McDonald, D. A. (1974). *Blood Flow in Arteries*. Edward Arnold, London
- Nielsen, J. Hedeholm, R.B., Heinemeier, J., Bushnell, P.G., Christiansen, J.S., Olsen, J., Ramsey, C.B., Brill, R.W., Simon, M., Steffensen, K.F. and Steffensen, J.F.

- (2016). Eye lens radiocarbon reveals centuries of longevity in the Greenland shark (*Somniosus microcephalus*). *Science* 353: 702-704.
- Priede, I.G. (1976). Functional morphology of the bulbus arteriosus of rainbow trout (*Salmo gairdneri* Richardson). *J. Fish Biol.* 9: 209-216.
- Randall, D.J. (1970). The circulatory system. *Fish Physiology* (Eds. W.S. Hoar and D.J. Randall) 4:133-172.
- Rhodin, J.A.G. (1972). Fine structure of elasmobranch arteries, capillaries and veins in the spiny dogfish, *Squalus acanthias*. *Comp. Biochem. Physiol. A.* 42: 59-64.
- Roach, M. R. and Burton, A. C. (1957). The reason for the shape of the distensibility curves of arteries. *Can. J. Biochem. Physiol.* 35: 181–190.
- Satchell, G. H. (1971). Circulation in Fishes. Cambridge Monographs in Experimental Biology No. 18. Cambridge: Cambridge University Press. 131pp.
- Shadwick, R.E. (1995). Mechanical organization of the mantle and circulatory system of cephalopods. *Mar. Freshwater Behav. Physiol.* 25: 69-85.
- Shadwick, R.E. (1998). Elasticity in arteries. *Amer. Sci.* 86: 535-541.
- Shadwick, R.E. (1999). Mechanical design in arteries. *J. Exp. Biol.* 202: 3305-3313.
- Shadwick, R.E. and Gosline, J.M. (1981). Elastic arteries in invertebrates, mechanics of the octopus aorta. *Science* 213:759–761.
- Shadwick, R.E. and Gosline, J.M. (1985). Mechanical properties of the octopus aorta. *J. Exp. Biol.* 114: 259–284.
- Shadwick, R.E., Pollock, C.M. and Stricker, S.A. (1990). Structure and biomechanical properties of crustacean blood vessels. *Physiol. Zool.* 63: 90–101.
- Skomal, G.B., Benz, G.W., 2004. Ultrasonic tracking of Greenland sharks, *Somniosus microcephalus*, under Arctic ice. *Mar. Biol.* 145: 489–498.
- Speers-Roesch B., Brauner, C.J., Farrell, A.P., Hickey, A.J.R., Renshaw, G.M.C., Wang, Y.S. and Richards, J.G. (2012). Hypoxia tolerance in elasmobranchs. II. Cardiovascular function and tissue metabolic responses during progressive and relative hypoxia exposures. *J. Exp. Biol.* 215:103-114.
- Stenslkken, K. O., Sundin, L., Renshaw, G. M. and Nilsson, G. E. (2004). Adenosinergic and cholinergic control mechanisms during hypoxia in the epaulette shark (*Hemiscyllium ocellatum*), with emphasis on branchial circulation. *J. Exp. Biol.* 207: 4451-4461.
- Stevens, E. D. and Randall, D. J. (1967). Changes in blood pressure, heart rate, and breathing rate during moderate swimming activity in rainbow trout. *J. Exp. Biol.* 46: 307-315.
- Taylor, E.W., Short, S. and Butler, P.J. (1977). The role of the cardiac vagus in the response of the dogfish *Scyliorhinus canicula* to hypoxia. *J. Exp. Biol.* 70:57-75.

- Watanabe, Y.Y., Lydersen, C., Fisk, A.T. and Kovacs, K.M. (2012). The slowest fish: Swim speed and tail-beat frequency of Greenland sharks. *J. Exp. Mar. Biol. Ecol.* 426-427: 5-11.
- Wong, L.C.Y. and Langille, B.L. (1996). Developmental remodeling of the internal elastic lamina of rabbit arteries. *Circ. Res.* 78: 799-805.

Figures

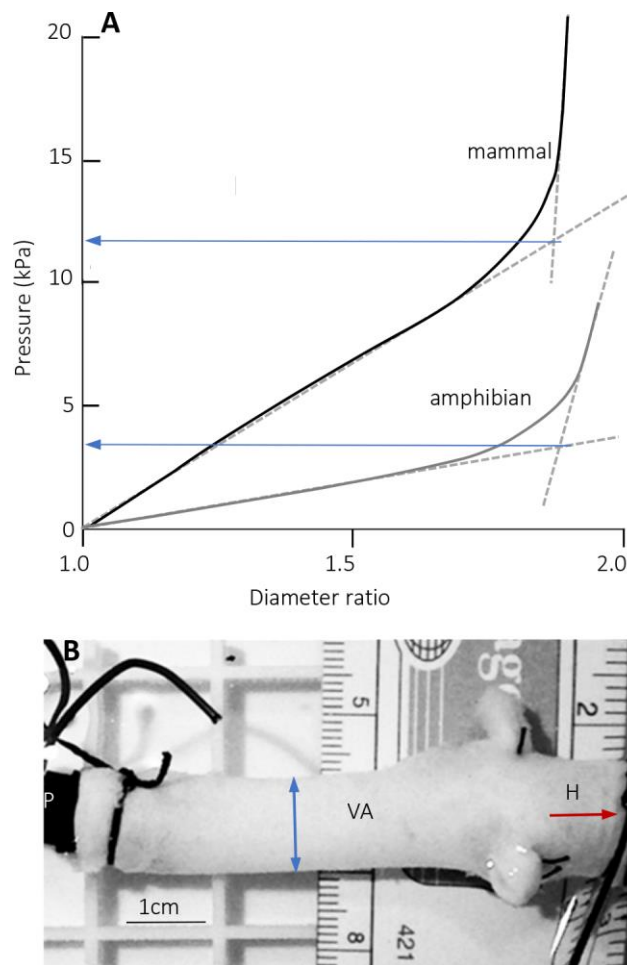


Fig. 1. A. Pressure vs. external diameter ratio for the aortas from a mammal (rat) and an amphibian (toad). The steepness of the curve indicates the stiffness of the artery wall. In both cases the aortas exhibit a two-part response approximated by two straight lines whose intersection (arrows) are close to the *in vivo* blood pressure (12kPa in the rat, 4kPa in the toad). B. Experimental set-up to inflate shark ventral aorta (VA), measuring pressure via a transducer port in the distal cannula (P) and diameter at the location of the blue arrow. Right end is proximal to heart (H, red arrow). Data for A taken from Gaballa et al., 1998 and Gibbons and Shadwick, 1991.

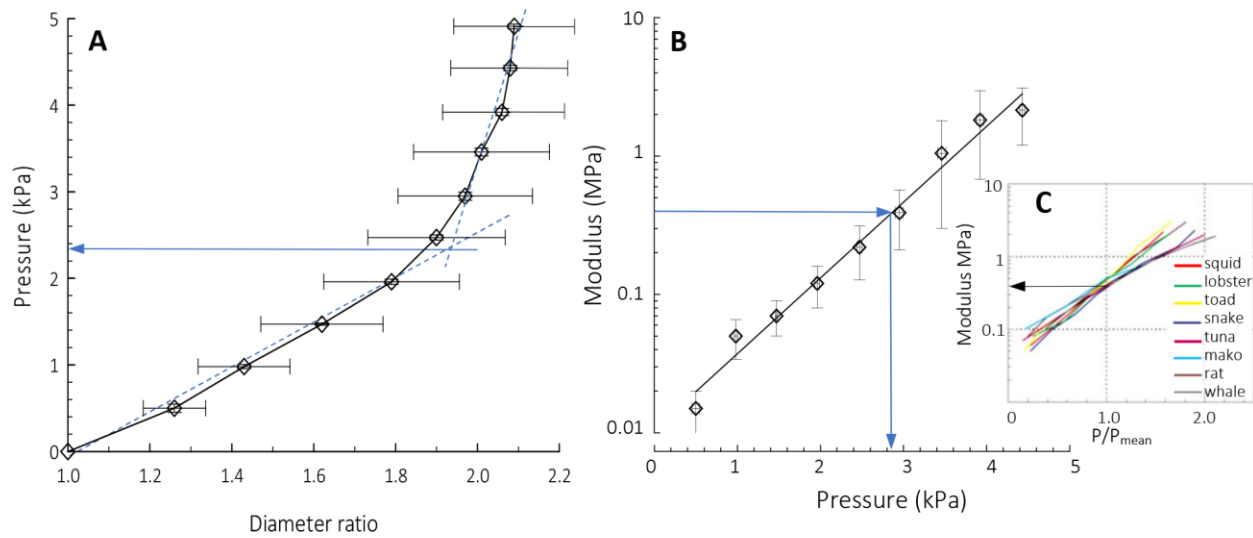


Fig. 2. A. Inflations of VAs from six Greenland sharks showing mean values of diameter ratio for a series of pressure increments from 0 – 5kPa. Linear regressions are shown for the first five data points ($R^2 = 0.994$) and last five data points ($R^2 = 0.933$). Their intersection is the transition from the aorta being compliant to stiff, and occurs at approximately 2.3kPa (arrow). B. Circumferential elastic modulus of the VA vs. inflation pressure, calculated from data in 2A ($R^2 = 0.975$). C. Elastic modulus of aortas from various vertebrates and invertebrates with closed circulatory systems vs. pressure normalized to the resting blood pressure of each species, P/P_{mean} (Shadwick, 1999). At mean blood pressure the modulus falls in the region of 0.3-0.5MPa in all cases (arrow). Referring back to 2B, if modulus is assumed to be 0.4MPa (horizontal arrow), the resting blood pressure is predicted to be 2.8kPa (vertical arrow). Data in C from Shadwick (1999).

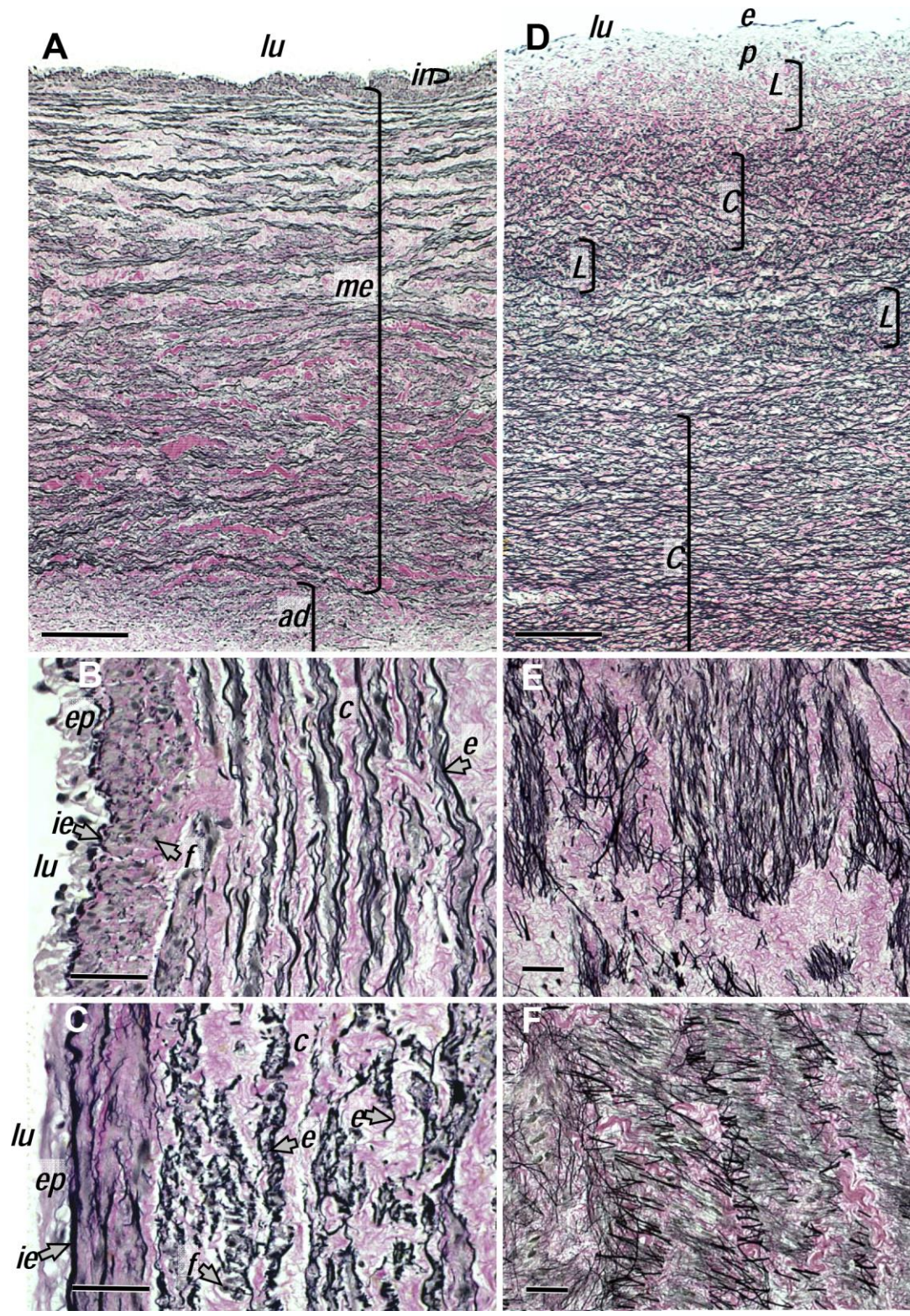


Fig 3. Histology of the VA of *S. microcephalus* (A-C,E,F) and *I. oxyrinchus* (D) showing elastin (e: black) and collagen (c: pink). A. Transverse section showing lumen (*lu*) at top, intima (*in*), media (*me*), adventitia (*ad*). Higher magnification transverse (B) and longitudinal (C) views showing epithelium (*ep*), internal elastic lamina (*ie*) and fibroblasts (*f*). These demonstrate that elastin fibres in the *ie* and the region next to it are predominantly longitudinal, but are circumferential in deeper regions. Sagittal sections (long axis in the horizontal direction) show elastin fibres oriented circumferentially (E) and longitudinally (F) at different depths. D. Transverse section of the VA of *I. oxyrinchus* showing a higher density of elastin fibres than in A, a partially disrupted epithelium, and no evidence of an internal elastic lamina. The wall is thicker than in *S. microcephalus* so the adventitia is not shown. Elastin fibres are oriented primarily circumferentially (C), but longitudinally (L) in some areas. Scale bars are 250 μ m in A,D and 50 μ m in others.